1P2-5

Proceedings of Symposium on Ultrasonic Electronics, Vol. 34 (2013) pp. 45-46
20-22 November, 2013

Investigation of Radiated ultrasound from electroacoustic transformation device –Thermophone-
電気音響変換素子-Thermophone-の放射音場に関する検討

Takuya Nishioka[1†], Yu Teshima[1], Takashi Mano[2], Ken Sakai[2], Takaaki Asada[2], Mami Matsukawa[1], Tetsuo Ota[1], and Shizuko Hiryu[1]
([1]Doshisha Univ.; [2]Murata Manufacturing Co., Ltd.)
西岡　卓哉 [1†], 手嶋　優風 [1], 間野　孝 [2], 酒井　賢 [2], 浅田　隆昭 [2], 松川　真美 [1],
太田　哲男 [1], 飛龍　志津子 [1]（[1]同志社大, [2]村田製作所）

1. Introduction

The thermophone is an electroacoustic transformation device which has simple and miniature structure to generate a sound wave without any mechanical vibration [1,2]. Conventionally, as a transducer for object detection in air, the narrow-band piezoelectric device using resonance characteristics is widely used. However, high time resolution using broadband frequency information will be required for ranging and detecting object shape with high precision.

In this paper, we first investigated the internal structure of the device using Scanning Electron Microscope (SEM) as well as measurements of acoustical characteristics to understand mechanisms of electroacoustic transformation of the thermophone. The relationship between the generated sound pressure level and the input electric power was measured. Directivity pattern and frequency characteristic were also investigated.

2. Ultrasonic radiation principle

A thermophone consists of three layers: a heat insulating and releasing layers in the back of a surface metallic film. The heat insulating layer insulates the AC component of the Joule heat generated on the metallic thin film to effectively propagate it to the air as a sound wave. On the other hand, the DC component of the heat propagates into the heat releasing layer. Here, when the alternating current ($I_m \sin 2\pi f_0 t$) is supplied to the metallic thin film of a thermophone, temperature (T) of the minute air parcel near the film surface is given by [1]

$$0.24(I_{\mathrm{m}} \sin 2\pi f_0 t)^2 \mathrm{R} = 2\alpha\beta\mathrm{T} + \alpha\gamma \frac{\mathrm{d}T}{\mathrm{d}t} \quad (1)$$

According to equation (1), the temperature change (ΔT) can be written by

$$\Delta T = \frac{0.12 I_{\mathrm{m}}{}^2 \mathrm{R}}{2\alpha\sqrt{\beta^2+\gamma^2\omega^2}} \cos\left(2\times 2\pi f_0 t + \tan^{-1}\frac{\gamma\omega}{\beta}\right) \quad (2)$$

The sound pressure $P(t)$ excited from a thermophone at distance r is:

$$P(t) = \frac{\mathrm{R}I_{\mathrm{m}}{}^2 \rho_0 \sqrt{2\times 6.0\times 10^{-11}\times 2f_0}}{r\gamma} \cos(2\times 2\pi f_0 t - \theta) \quad (3)$$

where R and α are resistance and area of a metallic thin film with thickness γ, β and c are thermal conductivity and capacity of the metallic thin film, ρ_0 is density of air, θ is phase difference.

3. Methods & Measurements

3.1 Experimental setup of SEM

As a pretreatment, a plane section of the thermophone was coated with Carbon and Platinum. The detailed structure was investigated by SEM (JSM-7500FD) using secondary and reflection electron images. Accelerating voltage was set at 12, 15 and 20 kV, respectively. Element analysis was conducted by XMA (JED-2300).

3.2 Observing ultrasonic radiation

The input voltage generated from the oscillator (Agilent, 33250A) was amplified (NF, HAS-4101), and then supplied to the thermophone (R = 60Ω). The sound waves were measured by a condenser microphone (B&K, 4939) set at 5 cm from the thermophone. The signals were amplified by 68 dB and high-pass filtered (NF, 3625, f = 10 kHz), and were observed using an oscilloscope (TDS 2024C). Horizontal and vertical directivity patterns of radiated sound waves were measured for the range of ±90 degrees by 5-degree step. The frequency characteristic of the thermophone was also measured up to 150 kHz.

4. Result

The SEM image shows that the thermophone consists of three layers: a metallic film, a heat insulating and a heat releasing layers (Fig. 1). The metallic film mainly consisting of Ag-Pd alloy particles, and heat insulating and releasing layers consist of glass and alumina, respectively (Table 1). Figure 2 shows input current signal (top) and observed sound waveform (bottom). Since the sound pressure level was proportion to the input

E-mail: shiryu@mail.doshisha.ac.jp

electric power, RI_m^2 (Fig. 3), the frequency of generated sound waves of the thermophone was $2f_0$. Figure 4 shows that the thermophone has a wide frequency range up to 150 kHz (the decrease over 100 kHz was due to the characteristics of the microphone used). In addition, we confirmed that directivity patterns show good agreement with theoretical estimations assuming a rectangular diaphragm with the size of the metallic film (Fig. 5).

5. Discussion and conclusion

The thermophone showed a broadband frequency characteristic. On the other hand, the conversion efficiency of the thermophone was estimated to be approximately 4.4×10^{-6} %, which should be improved for practical applications. Shinoda et al. has reported that the conversion efficiency is related to the ratio of the products of thermal capacity and conductivity between the heat insulating and releasing layers [3]. Based on the element analysis of XMA, the ratio of our thermophone can be estimated as heat releasing layer : heat insulating layer = 230 : 1, which is smaller than those of other electroacoustic transformation devices [3,4]. Other than manipulating physical properties of compositions for each layer, increasing the thickness of a heat releasing layer appears to be one of the practical solutions to improve the conversion efficiency.

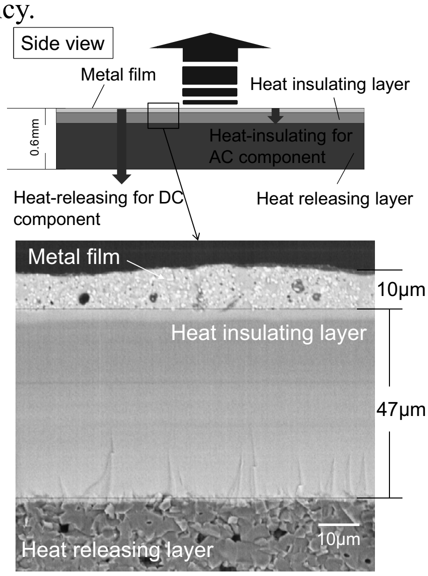

Fig. 1 Sectional view of Thermophone.

Table1 composing element of metal film, heat insulating layer and heat releasing layer.

Metal film		Heat insulating layer		Heat releasing layer	
Element	Molar ratio (%)	Element	Molar ratio (%)	Element	Molar ratio (%)
Si	39.47	Si	71.19	Al	93.5
Pd	14.38	Al	17.21	Si	5.4
Si,Al,Ag,Pd	46.15	Ca,Ba,La	11.60	Ca	1.1

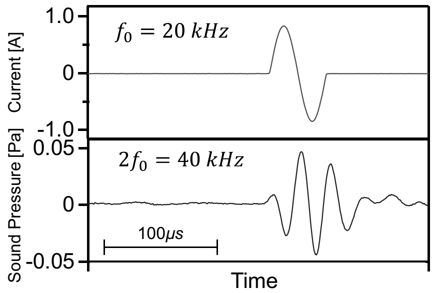

Fig. 2 Input current signal (top) and radiated sound wave (bottom) from the thermophone.

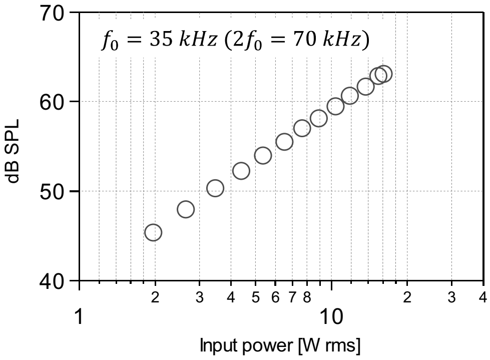

Fig. 3 Relationship between input power and sound pressure level of radiated sound wave from the thermophone.

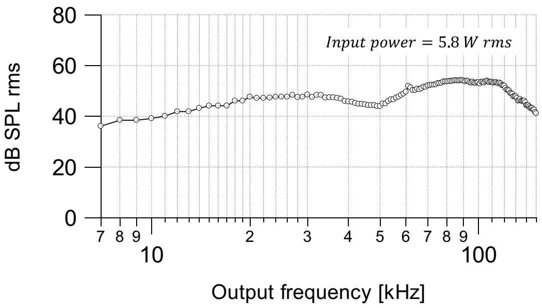

Fig. 4 Frequency characteristics of the thermophone.

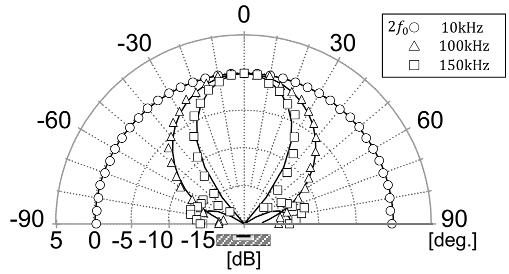

Fig. 5 Directivity patterns of radiated sound wave from the thermophone (solid lines indicate theoretical estimations assuming rectangular diaphragm).

References

1. H. D. Arnold and I. B. Crandall, "The thermophone as a precision source of sound," Phys. Rev., vol. 10, pp. 22-38, 1917.
2. E. C. Wente, "The thermophone," Phys. Rev., vol. 19, pp. 333-345, 1922.
3. H. Shinoda et. al., "Thermally induced ultrasonic emission from porous silicon," Nature, vol. 400, pp.853-855, 1999.
4. L. Xiao, et. al., "Flexible, stretchable, transparent carbon nanotube thin film loudspeakers," NanoLett., Vol. 8, pp. 4539-4545, 2008.